Low Temperature Physics/Fizika Nizkikh Temperatur, 2016, v. 42, No. 8, pp. 887–891

Surface plasmon-polariton resonance at diffraction of THz radiation on semiconductor gratings

I.S. Spevak[1], A.A. Kuzmenko[1], M. Tymchenko[1], V.K. Gavrikov[2], V.M. Shulga[2], J. Feng[3], H.B. Sun[3], Yu.E. Kamenev[1], and A.V. Kats[1]

[1]*O. Ya. Usikov Institute for Radiophysics and Electronics of the National Academy of Sciences of Ukraine*
12 Ac. Proskury, Kharkiv 61085, Ukraine
E-mail: stigan@rambler.ru

[2]*Institute of Radio Astronomy of the National Academy of Sciences of Ukraine*
4, Chervonopraporna, Kharkiv 61002, Ukraine

[3]*Jilin University, 2699 Qianjin Str., Changchun 130012, China*

Received March 16, 2016, published online June 24, 2016

Resonance diffraction of THz hydrogen cyanide laser radiation on a semiconductor (InSb) grating is studied both experimentally and theoretically. The specular reflectivity suppression due to the resonance excitation of the THz surface plasmon-polariton is observed on a pure semiconductor grating and on semiconductor gratings covered with a thin dielectric layer. The dielectric coating of the grating results in the resonance shift and widening depending both on the layer thickness and dielectric properties. A simple analytical theory of the resonance diffraction on rather shallow gratings covered with a dielectric layer is presented, and the results are in a good accordance with the experimental data. Analytical expressions for the resonance shift and broadening are essential for the resonance properties understanding and useful for sensing data interpretation of the agents deposited on the grating surface.

PACS: 42.25.Fx Diffraction and scattering.

Keywords: plasmon-polariton, semiconductor, resonance, diffraction, grating.

The terahertz band (0.3–10 THz) is a very promising frequency range of the electromagnetic spectrum due to a wide variety of possible applications such as imaging, nondestructive evaluation, biomedical analysis, chemical characterization, remote sensing (including detection of agents associated with illegal drugs or explosives), communications, etc [1–3]. Therefore, in spite of the lack of cheap and compact THz sources and detectors, fundamental and applied researches in the THz area are a problem of today.

Imaging and sensing capabilities of the THz radiation can be substantially enhanced by employing the surface plasmon-polariton (SPP) owing to its high field concentration near a metal-dielectric interface. SPPs are transverse magnetic waves that propagate along the boundary between the conducting and dielectric media and are coupled to the collective oscillations of free electrons in a conductor [4]. In the visible and IR ranges metals are usually considered as standard SPP supported media. In contrast to this, in the THz region metals behave as approximately perfect conductors that results in a weak SPP localization within the adjacent dielectric and a huge free path length. Actually, the terahertz SPP at a flat metal loses its surface nature and its existence calls into question.

Meanwhile, many semiconductors possess optical properties allowing efficient THz SPP excitation, propagation and manipulation without any additional treatment [5–8]. It is due to the fact that the dielectric permittivity of these semiconductors in THz is analogous to that of metals in the visible spectrum range. So, all effects observed in optics and associated with SPP, in particular, total suppression of the specular reflection [9,10], resonance polarization transformation [11–13], enhanced transmission through optically thick structured metal layers [14,15], and its counterpart, suppressed transmission through optically thin structured metal films [16–19], can be realized in the THz region with application of SPP. An additional advantage of semiconductors as plasmon-polariton supporting media is related to

© I.S. Spevak, A.A. Kuzmenko, M. Tymchenko, V.K. Gavrikov, V.M. Shulga, J. Feng, H.B. Sun, Yu.E. Kamenev, and A.V. Kats, 2016

the fact that their optical parameters can be controlled by optical excitation or thermal action [20–22].

A majority of recent THz experiments are carried out by using the common terahertz time-domain setup [5,6,23,24,26] with a pulse broadband THz source. The typical full angle divergence of the THz beam is ~ 0.1 rad and the spectral resolution of the setup is $\sim 6...18$ GHz [23–26]. At the same time, the spectral half-width of the SPP resonance on a shallow ($b/d \le 0.1$, where b is the grating depth, d is the period) semiconductor grating is usually about ≤ 5 GHz, and the angular half-width of the resonance is ~ 0.01 rad. Evidently, a more collimated THz beam and better spectral resolution of the experimental setup are needed for detailed study of the SPP resonance's fine structure, and the THz laser is the most suitable tool for this purpose.

In this article we investigate the resonance diffraction of the HCN (hydrogen cyanide) laser radiation (the wavelength λ = 336.6 μm) on the InSb grating (dielectric permittivity at room temperature [27] $\varepsilon = -87 + 37.8i$, where i stays for the imaginary unity). The quality of the conical laser beam is characterized by the spectral width 30 kHz; the full angular width (approximately Gaussian-profiled) is $\simeq 0.01$ rad ($\simeq 0.9$ deg).

Four gratings produced successively by the standard lithographic process from a single 0.8 mm thick InSb wafer were under consideration. Namely, the first experiment was performed with the initial grating (without removing the photoresist). The following experiment was performed with the second grating resulting from the first one after subsequent etching, so this grating had deeper grooves. The third grating was obtained by subsequent etching of the second one. As a result, all three gratings where of equal period, d = 254 μm, but were of different grooves' depth and width. Specifically, in all cases the grooves were of semi-elliptic profile with the semi-axes (a,b) equal to $(53.5\,\mu\text{m}, 10\,\mu\text{m})$, $(65\,\mu\text{m}, 20\,\mu\text{m})$, $(71.5\,\mu\text{m}, 24\,\mu\text{m})$, respectively. Here $2a$ denotes the groove width, see Fig. 1, and the depth, b, is counted from the semiconductor surface. Finally, the fourth grating came out from the third one after removing the residual photoresist layer so that its period was the same as for other gratings, and its profile parameters, $(a,b) = (71.5\,\mu\text{m}, 24\,\mu\text{m})$, coincide with those for third grating.

The laser beam was p-polarized. Its intensity distribution was nearly Gaussian with the initial radius of 6.7 mm. The incidence plane was perpendicular to the grating's grooves and all diffracted beams also were in the incidence plane and are p-polarized, see Fig. 1.

The diffraction geometry was chosen so that the resonance takes place in the -1st diffraction order. In this case the only propagating diffraction beam is the specular reflected one. Owing to this, the radiative losses are minimal, resulting in maximizing the resonance strength and minimizing the resonance widening mostly caused by radiative losses.

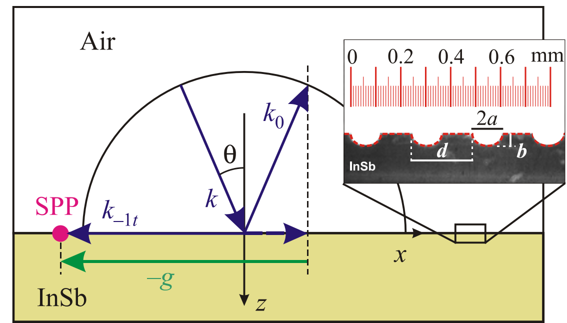

Fig. 1. (Color online) Geometry of the diffraction problem and the grating profile.

The experimental results are presented in Fig. 2. The well-marked suppression of the specular reflectivity is observed in a close vicinity of the Rayleigh angle, θ_R, $\sin\theta_R = \lambda/(\sqrt{\varepsilon_1}d) - 1$, where the -1st diffraction order transforms from the propagating wave ($\theta > \theta_R$) to the inhomogeneous ($\theta < \theta_R$) one. Here λ is the vacuum wavelength, ε_1 stays for the dielectric permittivity of the upper medium (air in our case). Under these conditions $\theta_R \simeq 19^\circ$. For all gratings the observed reflectivity minima correspond to the inhomogeneous -1st diffraction order that proves resonance SPP excitation. Note, that the reflectivity minima for the gratings with the residual photoresist are grouped near $\theta \approx 18^\circ$, while for the fourth (pure) grating, with the same profile and period as the third one has, the reflectivity lies aside, at $\theta \approx 18.5^\circ$. It is clear that this difference is due to presence of the photoresist on the grating surface. Besides the resonance shift,

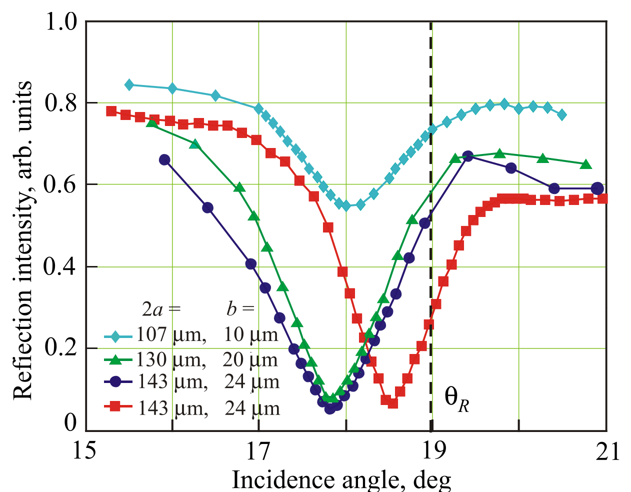

Fig. 2. (Color online) Experimental dependence of the specular reflectivity on the incidence angle. The grating parameters are indicated in the legend. The three initial curves correspond to the gratings with the residual photoresist. The fourth curve (red square markers) corresponds to the pure grating with the removed photoresist.

the photoresist layer increases the resonance width. The resonance width also increases with the grating depth.

A simple explanation of experimental results follows from the analytical theory [7,8,12,13]. Let a plane p-polarized wave, $\mathbf{H} = \mathbf{e}_y \exp[ik(\alpha_0 x + \beta_0 z)]$ (with $\alpha_0 = \sin\theta$, $\beta_0 = \cos\theta$, $k = \sqrt{\varepsilon_1}\omega/c$, where c denotes vacuum light speed, ω is the monochromatic wave angular frequency, k is a wavenumber in the upper halfspace, θ stays for the angle of incidence, see Fig. 1), is incident onto a periodically profiled surface, $z = \zeta(x)$, $\zeta(x) = \sum_n \zeta_n \exp(ingx)$, $g = 2\pi/d$, where d is the grating period. Then the amplitudes h_n of the diffracted waves, $h_n \exp[ik(\alpha_n x - \beta_n z)]$, with $\alpha_n = \alpha_0 + + ng/k$, $\beta_n = \sqrt{1-\alpha_n^2}$, where the square root branch is chosen so that $\mathrm{Re}, \mathrm{Im}\,(\beta_n) \ge 0$ for real-valued α_n, are

$$h_r = (1+R)\nu_{r0}/\Delta_r, \quad \Delta_r = b_r + \Gamma_r, \tag{1}$$

$$h_N = R\delta_{N0} + \frac{1+R}{b_N}\nu_{N0} + \frac{1}{b_N}\left(\nu_{Nr} + \sum_M \frac{\nu_{NM}\nu_{Mr}}{b_M}\right)h_r, \tag{2}$$

where $b_m = \beta_m + \xi$, $R = (\beta_0 - \xi)/(\beta_0 + \xi)$ is the Fresnel reflection coefficient from a plane interface, the quantities $\nu_{mn} = ik(1-\alpha_m\alpha_n)\zeta_{m-n}$ are proportional to the $n-m$ Fourier harmonic of the grating, $\Gamma_r = \sum_{N\ne r} |\nu_{Nr}|^2 / b_N$. The indexes r and N, M correspond to the resonance (in our case $r = -1$) and nonresonance diffraction orders, respectively $(N, M \in \mathbb{Z}\backslash r$, $\mathbb{Z}$ stays for the set of integers), $\xi = \sqrt{\varepsilon_1/\varepsilon}$ is the relative surface impedance, ε is the dielectric permittivity of the semiconducting medium. The quantity Γ_r in the denominator of Eq. (1) takes into account scattering of the resonance diffraction order, h_r, into the nonresonance ones, h_N, and vice versa,

$$h_r \xrightarrow{\zeta_{N-r}} h_N \xrightarrow{\zeta_{r-N}} h_r. \tag{3}$$

It is supposed that Γ_r is a finite quantity owing to rather fast decrease of the profile Fourier harmonics, ζ_n, with $|n|$ increase, so the corresponding series converges. Generally speaking, Γ_r depends on the angle of incidence θ. But this dependence in the close resonance vicinity is weak, the relative variation is no more than 5% within the resonance width even for the deepest grating for which $|\Gamma_r|$ achieves its maximal value. Therefore, for estimations we can take Γ_r at the Rayleigh angle, $\theta = \theta_R \simeq 19^\circ$.

The resonance condition resulting in $|h_r|^2$ maximization and consequent $|h_0|^2$ minimization is $\mathrm{Im}\,\Delta_r = 0$, or, explicitly, $\theta = \theta_{\mathrm{res}}$ with

$$\theta_{\mathrm{res}} = \arcsin\left\{-\frac{r\lambda}{\sqrt{\varepsilon_1}d} + \frac{r}{|r|}\sqrt{1 + \mathrm{Im}\,(\xi+\Gamma_r)^2}\right\}. \tag{4}$$

Emphasize, Eq. (4) predicting the resonance position for a plane wave with the resonance shift taken into account, give us the value that is in a good agreement with the experimental point for the clean (fourth) grating, cf. red (solid) curves in Figs. 2 and 3.

The full resonance width at the half-height can be obtained from Eq. (1) and in terms of the incident angle is

$$\Delta\theta = 2\mathrm{Re}\,(\xi+\Gamma_r)\,|\,\mathrm{Im}\,(\xi+\Gamma_r)\,|\,/\cos\theta. \tag{5}$$

According to Eq. (5), $\Delta\theta = 0.72^\circ$ for the clean (fourth) grating, while the experimental value is $\Delta\theta = 1.15^\circ$. Evidently, in the experiment the resonance experiences broadening caused by the incident beam angular divergence that is of order $\delta\theta = 0.9^\circ$. The latter value is comparable with the plane wave resonance width.

Note here that the dispersion relation of the SPP at a plane surface of highly conducting medium, $|\varepsilon| \gg 1$, is $q_{SPP}^2 = k^2(1-\xi^2)$, $\xi = \xi(\omega)$, where $q_{SPP} = q_{SPP}(\omega)$ is the complex-valued in-plane component of the SPP wavevector. For low losses, $\xi' \ll |\xi''|$, the real part of q_{SPP} prevails essentially the imaginary one, i.e., the SPP path length, $L = 2\pi/(\mathrm{Im}\,q_{SPP})$, is much greater than the wavelength $\Lambda = 2\pi/(\mathrm{Re}\,q_{SPP}) \simeq \lambda$, $L \gg \Lambda$. It can be strictly obtained from the above general solution of the inhomogeneous problem, Eq. (1), together with the resonance condition, Eq. (4), corresponding to the scattering matrix pole, that the periodic corrugation results in a specific renormalization of the surface impedance,

$$\xi \to \bar{\xi} = \xi + \Gamma_r. \tag{6}$$

This renormalization leads to the shift and broadening of the SPP resonance as compared to those for a plane surface: the deeper the groves the greater the resonance shift and width. It is just the renormalized impedance, $\bar{\xi} = \xi + \Gamma_r$, stays in the denominator in Eq. (1). In turn,

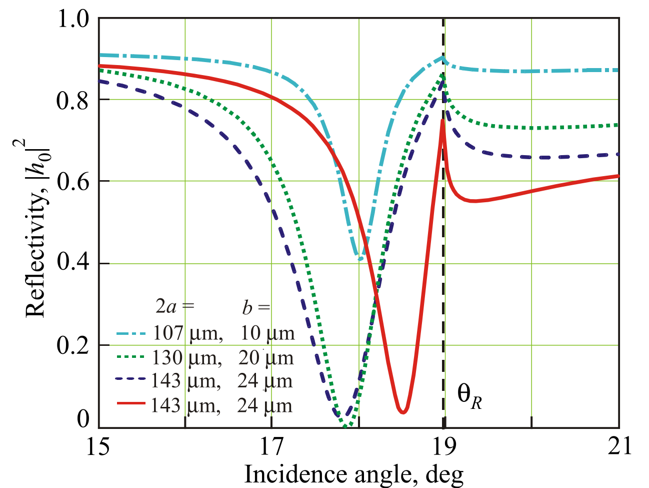

Fig. 3. (Color online) Dependence of the specular reflectivity on the incidence angle: theoretical results for a plane wave.

namely the renormalized impedance enters the SPP dispersion relation for profiled interfaces. It should be noted that $\mathrm{Re}\,\Gamma_r > 0, \mathrm{Im}\,\Gamma_r < 0$, that is their signs coincide with those of the surface impedance, $\mathrm{Re}\,\xi > 0$, $\mathrm{Im}\,\xi < 0$.

To explain the resonance shift and broadening due to the residual photoresist, consider that the photoresist covers the grating by a thin continuous layer. Supposing that the effects of the covering thin layer and corrugations are independent, we can use the dispersion relation for the SPP at a plane surface with a thin layer [4]. Simple considerations show that the effect of the layer with some dielectric permittivity ε_2 and small thickness ℓ as compared with the radiation wavelength, $k\ell \ll 1$, can be described by changing the relative surface impedance of the conductor adjacent to the semiinfinite dielectric, ξ, by some effective impedance value, $\tilde{\xi}$, i.e, one has to perform the following substitution

$$\xi \to \tilde{\xi} = \xi + G,\ \ G = -i\left(1 - \frac{\varepsilon_2}{\varepsilon}\right)\left(1 - \frac{\varepsilon_1}{\varepsilon_2}\right)k\ell. \qquad (7)$$

This expression is valid under the conditions $|\varepsilon| \gg \varepsilon_1$, $\sqrt{|\varepsilon_2/\varepsilon_1 - 1|}\, k\ell \ll 1$. There are no other limitations on ε_2 value, the ratio $\varepsilon_2/\varepsilon$ can be rather arbitrary. Noteworthy, for $\varepsilon_2 > \varepsilon_1$ the dielectric layer effects in the same direction as the corrugations do as far as $\mathrm{Re}\,G > 0$, $\mathrm{Im}\,G < 0$, i.e., their signs coincide with those of $\mathrm{Re}\,\Gamma_r$ and $\mathrm{Im}\,\Gamma_r$, respectively.

In the case of the corrugated surface covered with some dielectric layer, the plasmon-polariton dispersion relation can be obtained by independent accounting for the both factors discussed, i.e., $\xi \to \xi + \Gamma_r + G$. Respectively, in the diffraction problem under examination we have to change the resonance denominator as follows,

$$\Delta_r \to \beta_r + \xi + \Gamma_r + G. \qquad (8)$$

Consequent transformations are to be performed in Eqs. (4), (5) as well, resulting in

$$\theta_{\mathrm{res}} = \arcsin\left\{-\frac{r\lambda}{\sqrt{\varepsilon_1}d} + \frac{r}{|r|}\sqrt{1 + \mathrm{Im}\,(\xi + \Gamma_r + G)^2}\right\}, \qquad (9)$$

$$\Delta\theta = 2\mathrm{Re}\,(\xi + \Gamma_r + G)\,|\,\mathrm{Im}\,(\xi + \Gamma_r + G)\,|\,/\cos\theta. \qquad (10)$$

The theoretical results obtained are presented in Fig. 3 for $\varepsilon_1 = 1$, $\varepsilon_2 = 2.6$ and the layer thickness $\ell = 6\ \mu\mathrm{m}$ (this value gives the best agreement with the corresponding experimental data).

To make the picture transparent we present here the characteristic values: $\xi = 0.021 - 0.101i$, $G = 0.0008 - 0.071i$, and $\Gamma_r(\theta_R) = 0.004 - 0.007i; 0.021 - 0.019i; 0.031 - 0.024i$ for the three successive gratings. The imaginary parts of these quantities determine the resonance position, see Eqs. (4), (9). As one can see, the resonance shift caused by the thin covering layer is greater than that owing to the corrugations. The real parts are responsible for the losses (both active and radiative ones caused by the diffraction) and, consequently, determine the resonance width, see Eqs. (5), (10). Although the layer is transparent (ε_2 is real) and does not actually absorb the radiation, the field tightening to the grating surface due to the layer existence results in additional grating absorption and considerable broadening of the resonance. Analytically it is manifested by the product of the real and imaginary parts of the renormalized impedance, see Eq. (10). Thus, for the deepest grating with the photoresist layer (the third one) the plane wave resonance width is about 1°, as opposed to 0.7° for the clean (uncovered) grating; meanwhile in the experiment these parameters appear to be 1.5°, and 1.15°, respectively. The difference is caused by finite value of the beam angular divergence.

Thus, the theory with the renormalized resonance denominator successfully describes the resonance shift conditioned by the covered layer and corrugations. However, the resonance width for a plane wave is evidently smaller than the experimental one for the restricted beam. To estimate the latter theoretically we have to take into account the angular spectrum of the incident beam in the framework of the theory presented.

To illustrate qualitatively the resonance diffraction features caused by the finite space spectrum of the incident beam we present in Fig. 4 the results of the numerical calculations for a plane beam (restricted only in xOz plane). The beam was supposed to be p-polarized, the plane of incidence was xOz. The beam profile was taken in the

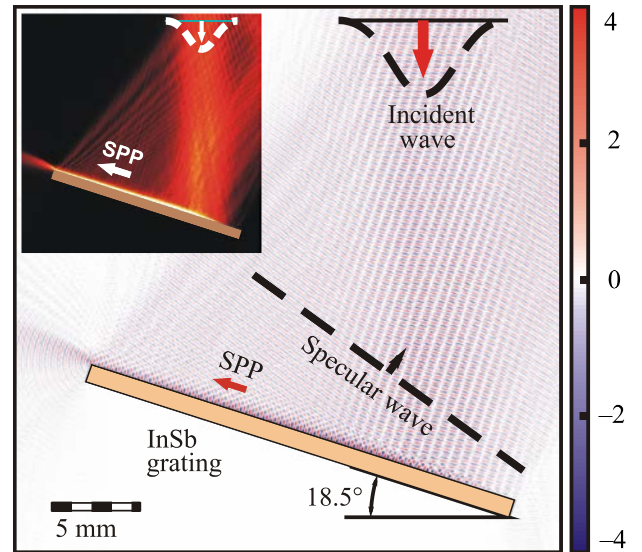

Fig. 4. (Color online) The space distribution of the magnetic field for the resonance diffraction of the restricted beam on the clean grating. The angle of incidence θ = 18.5° is chosen so that to result in the specular reflectivity minimum. The main picture presents the instantaneous field distribution, and the time averaged intensity distribution is shown in the inset. The model calculations where performed for a "plane" beam (i.e., restricted in xOz plane only).

Gaussian form with initial space width 6.7 mm and the characteristic angular width 0.9°. The strict numerical calculations were performed with COMSOL. The instantaneous and time averaged space dependencies of the squared magnetic field are shown. Notice high enhancement of the field near the interface that corroborates the SPP excitation. Within the laser spot area the SPP magnitude experiences increase in the propagation direction (to the left). It can be also seen that the SPP excited propagates along the grating outside the limits of the laser spot also. This is in accordance with the estimation of its free path length. The latter is of order $25\lambda \simeq 8.4$ mm. As a matter of fact, outside the highlighted spot the runaway SPP is efficiently rescattered into the specular direction. This, in turn, results in noticeable negative displacement of the specularly reflected beam, the so called Goos-Hänchen effect [28,29].

In conclusion, we have investigated both theoretically and experimentally the resonance suppression of the specular reflection of the THz laser radiation from semiconductor gratings. It was shown that covering the grating with a thin transparent layer results in the resonance shift and broadening. The theoretical relations obtained could be used for studying the surface properties and agents deposited on the grating surface.

This work was supported by the Ukrainian State program "Nanotechnologies and nanomaterials", and by the program of the National Academy of Sciences of Ukraine "Fundamental problems of nanostructured systems, nanomaterials and nanotechnologies".

1. M. Tonouchi, *Nature Photonics* **1**, 97 (2007).
2. W.L. Chan, J. Deibel, and D.M. Mittleman, *Rep. Progr. Phys*. **70**, 1325 (2007).
3. X.-C. Zhang and J. Xu, *Introduction to THz Wave Photonics*, Springer, New York (2010).
4. H. Raether, *Surface Plasmons on Smooth and Rough Surfaces and on Gratings*, Springer, Berlin (1988).
5. J.G. Rivas, M. Kuttge, P.H. Bolivar, and H. Kurz, *Phys. Rev. Lett.* **93**, 256804 (2004).
6. M. Kuttge, H. Kurz, J.G. Rivas, J.A. Sanches-Gill, and P.H. Bolivar, *J. Appl. Phys*. **101**, 023707 (2007).
7. N.A. Balakhonova, A.V. Kats, and V.K. Gavrikov, *Appl. Phys. Lett*. **91**, 113102 (2007).
8. I.S. Spevak, M.A. Timchenko, V.K. Gavrikov, V.M. Shulga, J. Feng, H.B. Sun, and A.V. Kats, *Appl. Phys. B, Lasers and Optics* **104**, 925 (2011).
9. M.C. Hutley and D. Maystre, *Opt. Commun*. **19**, 431 (1976).
10. G.M. Gandelman and P.S. Kondratenko, *JETP Lett.* **38**, 246 (1983).
11. S.J. Elston, G.P. Bryan-Brown, and J.R. Sambles, *Phys. Rev. B* **44**, 6393 (1991).
12. A.V. Kats and I.S. Spevak, *Phys. Rev. B* **65**, 195406 (2002).
13. A.V. Kats, I.S. Spevak, and N.A. Balakhonova, *Phys. Rev. B* **76**, 075407 (2007).
14. T.W. Ebbesen, H.J. Lezec, H.F. Ghaemi, T. Thio, and P.A. Wolff, *Nature* **391**, 667 (1998).
15. F.J. Garsia-Vidal, L. Martin-Moreno, T.W. Ebbesen, and L. Kuipers, *Rev. Mod. Phys*. **82**, 729 (2010).
16. I.S. Spevak, A.Yu. Nikitin, E.V. Bezuglyi, A. Levchenko, and A.V. Kats, *Phys. Rev. B* **79**, 161406(R) (2009).
17. J. Braun, B. Gompf, G. Kobiela, and M. Dressel, *Phys. Rev. Lett*. **103**, 203901 (2009).
18. S. Xiao, J. Zhang, C. Jeppesen, R. Malureanu, A. Kristensen, and N.A. Mortensen, *Appl. Phys. Lett*. **97**, 071116 (2010).
19. G. D'Aguanno, N. Mattiucci, A. Alù, and M.J. Bloemer, *Phys. Rev. B* **83**, 035426 (2011).
20. J.G. Rivas, M. Kuttge, H. Kurz, P.H. Bolivar, and J.A. Sanches-Gill, *Appl. Phys. Lett*. **88**, 082106 (2006).
21. J.A. Sanches-Gill and J.G. Rivas, *Phys. Rev. B* **73**, 205410 (2006).
22. J.G. Rivas, J.A. Sanches-Gill, M. Kuttge, P.H. Bolivar, and H. Kurz, *Phys. Rev. B* **74**, 245324 (2006).
23. Ch. Fattinger and D. Grischkovsky, *Appl. Phys. Lett*. **54**, 490 (1989).
24. D. Qu and D. Grischkovsky, *Phys. Rev. Lett*. **93**, 196804 (2004).
25. M. Nazarov, J.-L. Coutaz, A. Shkurinov, and F. Garet, *Opt. Commun*. **277**, 33 (2007).
26. G. Gaborit, D. Armand, J.-L. Coutaz, M. Nazarov, and A. Shkurinov, *Appl. Phys. Lett*. **94**, 231108 (2009).
27. E.D. Palik, *Handbook of Optical Constants of Solids II*, Edward D. Palik (ed.), Academic, Boston (1998).
28. C. Bonnet, D. Chauvat, O. Emile, F. Bretenaker, A. Le Floch, and L. Dutriaux, *Opt. Lett*. **26**, 666 (2001).
29. K.Y. Bliokh and A. Aiello, *J. Opt*. **15**, 014001 (2013).